
Efficient Algorithm for Quantitative Assessment of Similarities among Atoms in Molecules

JERZY CIOSLOWSKI* and BORIS B. STEFANOV

*Department of Chemistry and Supercomputer Computations Research Institute,
Florida State University, Tallahassee, Florida 32306-3006*

PERE CONSTANS

Institut de Quimica Computacional, Universitat de Girona, Girona 17071, Spain

Received 5 July 1995; accepted 1 November 1995

ABSTRACT

A new algorithm for quantitative assessment of similarity between two atoms in molecules is presented. Both the atomic similarity index and its derivatives with respect to the three Euler angles that describe the mutual orientation of the atoms under comparison are computed efficiently by taking advantage of the recently developed analytical representations for atomic zero-flux surfaces. The use of such representations makes it possible to substantially enhance the accuracy of the computed similarity indices without increasing the cost of their evaluation. Numerical tests involving oxygen atoms in several carbonyl compounds demonstrate the ability of the new algorithm to discern small changes in atomic similarity that are brought about by second-neighbor effects. Comparisons among hydrogen atoms in the acrolein molecule reveal the usefulness of the similarity index in detection and quantification of the effects of steric interactions on atomic shapes. © 1996 by John Wiley & Sons, Inc.

Introduction

The concepts of transferable atoms and functional groups are the primary tools with which most of the progress in our understanding

of the chemical properties of matter has been achieved. The ubiquitous use of these intuitive concepts allowed researchers to systematize chemical reactions involving millions of diverse molecules long before the immense predictive power of quantum mechanics became available. In contrast, a rigorous quantum-mechanical theory of atoms in molecules has emerged only very recently thanks to the pioneering research of Bader.¹

* Author to whom all correspondence should be addressed.

The addition of a single postulate to the original formulation of quantum mechanics provides the means for discerning atoms within molecules. Attractor basins, i.e., regions in Cartesian space bordered by surfaces of zero flux in the field of the electron density gradient, possess all the properties of separate quantum-mechanical systems. Each of these regions is spanned by gradient paths [lines of the steepest ascent in the electron density $\rho(\mathbf{r})$] terminating at a single point called an attractor. When an attractor coincides with one of the nuclei present in the molecule in question X , the union of this nucleus and its attractor (or atomic) basin Ω_A defines an atom A in X .¹ The atomic zero-flux surface that delineates Ω_A may consist of one or more zero-flux surface sheets. These sheets, also known as interatomic surfaces, determine the shape of an atom within a molecule. Most atoms in molecules are seminfinite (i.e., they extend to infinity in at least one radial direction), whereas all atoms in crystals possess limited extents.

Like their intuitively defined counterparts, atoms in molecules can be combined into highly transferable functional groups. The transferability of such groups, which has been empirically demonstrated for the $-\text{CH}_2-$ fragment,² holds the promise of affording a route to a new class of electronic structure methods in which large systems (such as proteins) are constructed by docking fragments taken from small molecules.^{3,4} Quantitative taxonomy of atoms in molecules and the assessment of their transferability constitute the first steps in the development of such methods. These tasks call for an extensive use of atomic shape analysis.

Shapes of any objects, including those of atoms in molecules, can be characterized with descriptors based solely on geometrical considerations.⁵ However, shape descriptors that involve the electron density are clearly preferable because of their sensitivity to not only the geometries of the atomic zero-flux surfaces but also the details of the atomic charge distributions. A descriptor that measures the degree of similarity between two atoms A and B present in molecules X and Y , respectively, is obtained by maximizing the quantity⁶

$$S_{A(X), B(Y)} = \left[\frac{\int_{\Omega_{AB}} \rho_X(\mathbf{r}) d\mathbf{r}}{\int_{\Omega_A} \rho_X(\mathbf{r}) d\mathbf{r}} \right] \left[\frac{\int_{\Omega_{BA}} \rho_Y(\mathbf{r}) d\mathbf{r}}{\int_{\Omega_B} \rho_Y(\mathbf{r}) d\mathbf{r}} \right] \quad (1)$$

where $\Omega_{AB} = \Omega_{BA} = \Omega_A \cap \Omega_B$ is the intersection (in the set-theoretical sense) of the atomic basins Ω_A and Ω_B . The maximization, during which the

nuclei of A and B are kept in coalescence, is carried out with respect to the three Euler angles $(\theta_1, \theta_2, \theta_3)$ that parametrize the mutual orientation (given by the rotation matrix \hat{T}_{AB}) of Ω_A and Ω_B . The so-defined atomic similarity index is always positive and equals 1 only if Ω_A is identical with Ω_B .

In the past, practical applications of the above index have been hampered by the limited numerical accuracy of the atomic zero-flux surfaces and the substantial computational cost involved in the evaluation of integrals over atomic basins. However, the recent advent of the variational approach to the determination of zero-flux surface sheets^{7,8} and the introduction of the semianalytical integration algorithm⁹ have made fast and accurate analysis of atomic shapes feasible. In this paper we report on a new algorithm for the evaluation and maximization of the atomic similarity index, eq. (1), that takes advantage of these new developments.

The Algorithm

In the course of its optimization, the index $S_{A(X), B(Y)}$ is repeatedly calculated together with its gradient and Hessian with respect to the Euler angles $(\theta_1, \theta_2, \theta_3)$. Most of the computational effort associated with these calculations is spent on the evaluation of the integrals

$$\begin{aligned} I_{A(X)} &= \int_{\Omega_{AB}} \rho_X(\mathbf{r}) d\mathbf{r} \\ I_{B(Y)} &= \int_{\Omega_{BA}} \rho_Y(\mathbf{r}) d\mathbf{r} \end{aligned} \quad (2)$$

The integrals over atomic basins Ω_A and Ω_B , which have to be computed only once, are approximated by sums that arise from numerical angular quadratures. For example,

$$\begin{aligned} N_{A(X)} &= \int_{\Omega_A} \rho_X(\mathbf{r}) d\mathbf{r} \\ &\approx \sum_m w_{A,m} \int_{\{R_{A,m}\}} \rho_X(\mathbf{r}_A + R\mathbf{u}_{A,m}) R^2 dR \end{aligned} \quad (3)$$

where the sum runs over rays m that emanate from the nucleus of A located at \mathbf{r}_A .⁹ The sets of intervals $\{R_{A,m}\}$ that enter eq. (3) are defined by the property

$$R \in \{R_{A,m}\} \Rightarrow \mathbf{r}_A + R\mathbf{u}_{A,m} \in \Omega_A \quad (4)$$

These sets, together with the quadrature weights $w_{A,m}$ and the ray directions expressed as the unit vectors $\mathbf{u}_{A,m}$, are precomputed for a given atom with an algorithm described previously.⁸ The radial integrals over the sets of intervals $\{R_{A,m}\}$ are evaluated analytically.⁹

In principle, one could compute the integrals over the intersections of atomic basins, eq. (2), in an analogous way, i.e.,

$$I_{A(X)} \approx \sum_m w_{A,m} \int_{\{R_{A \cap B, m}\}} \rho_X(\mathbf{r}_A + R\mathbf{u}_{A,m}) R^2 dR \quad (5)$$

where

$$R \in \{R_{A \cap B, m}\} \Rightarrow \mathbf{r}_A + R\mathbf{u}_{A,m} \in \Omega_{AB} \quad (6)$$

However, since most of the sets $\{R_{A \setminus B, m}\}$,

$$R \in \{R_{A \setminus B, m}\} \Rightarrow (\mathbf{r}_A + R\mathbf{u}_{A,m} \in \Omega_A) \cap (\mathbf{r}_A + R\mathbf{u}_{A,m} \notin \Omega_B) \quad (7)$$

are empty for pairs of atoms that are not too dissimilar, the computation of the integrals is substantially faster when the expressions

$$I_{A(X)} = N_{A(X)} - \tilde{I}_{A(X)},$$

$$\tilde{I}_{A(X)} \approx \sum_m w_{A,m} \int_{\{R_{A \setminus B, m}\}} \rho_X(\mathbf{r}_A + R\mathbf{u}_{A,m}) R^2 dR \quad (8)$$

are used instead. Additional gains in performance result from the fact that the smallness of $\tilde{I}_{A(X)}$ allows for an efficient thresholding of primitive pairs in the radial integrations.⁹

In light of the above considerations, it is clear that the most efficient way of computing the atomic similarity index is to maximize $S_{A(X), B(Y)}$ expressed as [compare eqs. (3) and (8)]

$$S_{A(X), B(Y)} = \left(1 - \tilde{I}_{A(X)}/N_{A(X)}\right) \left(1 - \tilde{I}_{B(Y)}/N_{B(Y)}\right) \quad (9)$$

The adaptive numerical quadratures⁸ employed in the evaluation of $\tilde{I}_{A(X)}$, $N_{A(X)}$, $\tilde{I}_{B(Y)}$, and $N_{B(Y)}$ are capable of producing highly accurate values of $S_{A(X), B(Y)}$. The sets $\{R_{A \setminus B, m}\}$ and $\{R_{B \setminus A, m}\}$ needed in the calculations of $\tilde{I}_{A(X)}$ and $\tilde{I}_{B(Y)}$, respectively, are furnished by a collation algorithm. For each ray m , $\{R_{A \setminus B, m}\}$ (or $\{R_{B \setminus A, m}\}$) is constructed from the corresponding set $\{R_{A, m}\}$ (or $\{R_{B, m}\}$) and the intersections (if any) of the ray with the atomic

zero-flux surface of B (or A). These intersections can be easily determined thanks to the analytical representation of the zero-flux surface sheets.^{7,8} The J th surface sheet of the atom B is given by the equation

$$\eta_{B,J} = F_{B,J}(\xi, \phi) \quad (10)$$

where $F_{B,J}$ is an analytical function and

$$\xi = \xi_{B,J}(\mathbf{r}), \quad \phi = \phi_{B,J}(\mathbf{r}), \quad \eta = \eta_{B,J}(\mathbf{r}) \quad (11)$$

are suitable curvilinear coordinates (note that \mathbf{r} in the above set of equations refers to the coordinate system of the molecule Y that contains the atom B). The radial coordinate $Q_{A, Jmk}$ of the k th intersection of the m th ray of A with the J th surface sheet of B is equal to the k th root of the function

$$P_{A, Jm}(R) = \eta_{B,J}(\mathbf{r}) - F_{B,J}[\xi_{B,J}(\mathbf{r}), \phi_{B,J}(\mathbf{r})] \\ = \mathbf{r}_B + R\hat{T}_{AB}\mathbf{u}_{A, Jm} \quad (12)$$

where $\hat{T}_{AB} \equiv \hat{T}_{AB}(\theta_1, \theta_2, \theta_3)$ is the rotation matrix that describes the mutual orientation of A with respect to B . Similarly, $Q_{B, Jmk}$ is computed from the function

$$P_{B, Jm}(R) = \eta_{A,J}(\mathbf{r}) - F_{A,J}[\xi_{A,J}(\mathbf{r}), \phi_{A,J}(\mathbf{r})] \\ = \mathbf{r}_A + R\hat{T}_{BA}\mathbf{u}_{B, Jm} \quad (13)$$

where $\hat{T}_{BA} = \hat{T}_{AB}^{-1} = \hat{T}_{AB}^T$. Equations (12) and (13) are solved with a high performance unidimensional search procedure that has been described previously.⁸

An important advantage of the afore-described algorithm is that it allows for a straightforward evaluation of the derivatives of $S_{A(X), B(Y)}$ with respect to the Euler angles $(\theta_1, \theta_2, \theta_3)$. Inspection of eqs. (8) and (9) leads to the conclusion that, provided the gradients of $Q_{A, Jmk}$ and $Q_{B, Jmk}$ are available, these derivatives can be computed very cheaply without invoking the expensive radial integrations. The gradient components $\partial Q_{A, Jmk}/\partial \theta_i$ ($i = 1, 2, 3$) are readily calculated from the equation

$$(\partial Q_{A, Jmk}/\partial \theta_i)(\mathbf{S}^T \hat{T}_{AB} \mathbf{u}_{A, Jm}) \\ + Q_{A, Jmk} [\mathbf{S}^T (\partial \hat{T}_{AB}/\partial \theta_i) \mathbf{u}_{A, Jm}] = 0 \quad (14)$$

where

$$\begin{aligned} \mathbf{S} = & \nabla \eta_{B,j}(\mathbf{r}) - \partial F_{B,j}[\xi_{B,j}(\mathbf{r}), \phi_{B,j}(\mathbf{r})] / \partial \xi \nabla \xi_{B,j}(\mathbf{r}) \\ & - \partial F_{B,j}[\xi_{B,j}(\mathbf{r}), \phi_{B,j}(\mathbf{r})] / \partial \phi \nabla \phi_{B,j}(\mathbf{r}) \\ \mathbf{r} = & \mathbf{r}_B + Q_{A,jmk} \hat{T}_{AB} \mathbf{u}_{A,jm} \end{aligned} \quad (15)$$

which is produced by differentiation of eq. (12). A second differentiation furnishes the Hessian elements in an analogous way.

In the actual maximization runs, the gradient of $S_{A(X), B(Y)}$ with respect to $(\theta_1, \theta_2, \theta_3)$ is computed analytically at each optimization step, whereas the Hessian is computed only at the first step, inverted, and then updated with the Broyden-Fletcher-Goldfarb-Shanno (BFGS) formula¹⁰ in each Newton-Raphson iteration. The signs and magnitudes of the Hessian eigenvalues are controlled, and the step size is halved when an iteration fails to increase the value of $S_{A(X), B(Y)}$. Such a strategy furnishes a robust maximization procedure that is largely unaffected by the numerical noise associated with the use of a finite grid in angular quadratures over regions in Cartesian space bordered by complicated surfaces with cusps and seams. This noise, which has an insignificant effect on the similarity index itself and is only mildly detrimental to the accuracy of the similarity gradient, produces error flare-ups in the similarity Hessian evaluated at certain combinations of Euler angles.

Multiple maxima in $S_{A(X), B(Y)}$ are encountered in comparisons involving low-symmetry atoms with multiple surface sheets. In such cases, the above algorithm converges to the maximum that is closest to the starting point. A judicious choice of the initial vector $(\theta_1, \theta_2, \theta_3)$ motivated by "chemical intuition" is usually sufficient to assure convergence to the global maximum.

Numerical Examples

All the calculations described below were carried out with MP2/6-311G** electron densities computed for molecular geometries optimized at the same level of theory. The atomic basins were determined with methods described previously.^{7,8} The accuracy of 2×10^{-4} a.u. was requested for all atomic properties, resulting in angular quadratures with 2600–3900 grid points for hydrogens, 6300–7800 points for oxygens, and 7000–45,400 points for carbons.

In order to assess the performance of the present algorithm, the previously published comparisons⁶ between the hydrogen and carbon atoms in CH_4 and C_2H_4 were reexamined. The values of 85.41 and 98.25% were obtained for $S_{\text{C}(\text{CH}_4), \text{C}(\text{C}_2\text{H}_4)}$ and $S_{\text{H}(\text{CH}_4), \text{H}(\text{C}_2\text{H}_4)}$, respectively, in good agreement with those of 85.7 and 98.5% produced by the old, less accurate method. The similarity calculations confirmed the expectations of a relatively small fraction of the grid points being used by the angular integrations over the $\Omega_A \setminus \Omega_B$ and $\Omega_B \setminus \Omega_A$ regions. For example, in the $\text{C}(\text{CH}_4)$ versus $\text{C}(\text{C}_2\text{H}_4)$ run, the integrations over Ω_A and Ω_B involved 26,275 and 18,073 grid points, respectively, of which only ca. 10,500 and 9000 points were active in the evaluations of $\tilde{I}_{A(X)}$ and $\tilde{I}_{B(Y)}$. As a result, despite a tenfold increase in accuracy, calculations employing the present algorithm were found to be as fast as those using the old method.

Shapes of atoms in molecules are affected not only by their direct connectivities, but also by the number and nature of the second neighbors. This phenomenon is particularly pronounced for atoms with low electron densities (such as hydrogens) that are located in the proximity of "heavy" atoms. For example, the hydrogens in CH_4 and CHF_3 are only 95.1% similar.⁶ On the other hand, variations in shapes of atoms with large electron densities are much less discernible, necessitating the use of the present, more accurate atomic similarity algorithm [an improvement in accuracy being also necessitated by the fact that the similarity indices computed for heavy atoms tend to have a smaller deviation from the value of 1 because of contributions from core electrons dominating the integrals that enter eq. (1)]. Taking into account the complicated character of intramolecular interactions, the shape of a given type of atom is expected to correlate poorly with its properties such as charge or the kinetic energy.

The recent work on the transferability of the oxygen atom in carbonyl compounds¹¹ provides a good illustration of the above point. In the series consisting of the formaldehyde, acetaldehyde, acetone, acrolein, formamide, and carbon dioxide molecules, the kinetic energy of the oxygen atom varies by as much as 0.035 a.u. (or 22 kcal/mol), whereas the variation in charge amounts to 0.0979 (Table I). However, these differences in atomic properties are not fully reflected in the computed atomic surfaces. For example, the surfaces of the carbonyl group oxygens in acetaldehyde and

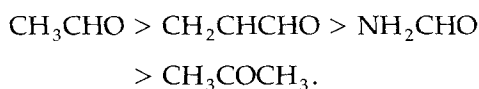
TABLE I.
Properties of Oxygen Atoms in Selected Carbonyl Compounds.

Molecule	Charge	Kinetic Energy ^a	Dipole Moment ^{a, b}
HCHO	-1.0324	75.7031	0.4929
CH ₃ CHO	-1.0608	75.7146	0.4834
CH ₃ COCH ₃	-1.0813	75.7206	0.4662
CH ₂ CHCHO	-1.0488	75.7001	0.4703
NH ₂ CHO	-1.1303	75.7348	0.4629
CO ₂	-1.0641	75.7342	0.6044

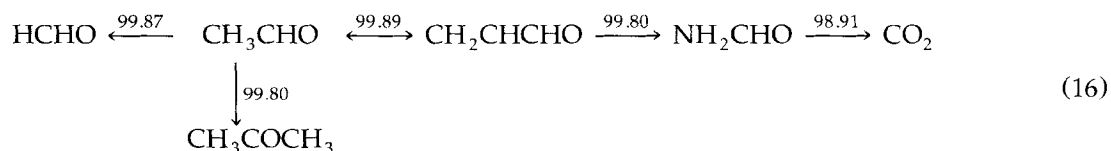
^a In atomic units.
^b Along the C=O bond.

acrolein are found to be remarkably similar by visual inspection, the dissimilarities present mostly in the surface portions far from the oxygen nuclei, despite the fact that their kinetic energies differ by 0.015 a.u. (or 9 kcal/mol). Thus, the variability in atomic properties appears to originate from differences in electron distributions in proximity to the attractor that barely affect the atomic shapes.

The computed values of the similarity index (Table II) support this interpretation. With the CO₂ molecule excluded, the similarities between the oxygen atoms exceed 99.5% in all instances. In other words, the shapes of these atoms approach the unattainable limit of perfect transferability^{12,13} quite closely. Still, the present calculations are sufficiently accurate to reveal interesting subtle trends in atomic similarities. These trends are in accordance with the expectations based on "chemical intuition." For example, the similarity to the oxygen atom in HCHO is found to decrease among the carbonyl group oxygens in the order



When one denotes by the symbols " $B \xrightarrow{S} A$ " a molecular pair such that the molecule B possesses the oxygen atom most similar (as measured by the value of the atomic similarity index S) to that in a given molecule A , the following graph emerges for the five compounds under study:



testifying to the strong resemblance among the carbonyl group oxygens in aldehydes. One should note that these trends in atomic similarities cannot be inferred directly from the atomic properties listed in Table I.

Multiple maxima in $S_{A(X), B(Y)}$ are encountered in calculations involving oxygen atoms with sufficiently low symmetries. The global maxima are attained at mutual orientations of atoms that produce the best matching of their second neighbors. Thus, for example, the best orientation in the O (acetaldehyde) versus O (acrolein) comparison corresponds to the matching of the "carbon sides" of each atom, whereas the secondary maximum ensues when the "carbon side" of one oxygen overlaps with the "hydrogen side" of the other. Interestingly, when a good match is impossible on both sides, the side with the better match prevails, producing a tilt in the respective direction. For instance, similarity between the oxygen atoms in HCHO and CH₃CHO is maximized when one of the atoms is rotated enough to furnish optimal matching between its "hydrogen side" and that of the other atom.

The case of hydrogen atoms in the acrolein molecule illustrates the application of the atomic similarity index to the detection and quantification of steric overcrowding in molecules. Among the four hydrogens, two (H₄ and H₇; Fig. 1) are subject to substantial steric congestion. The four zero-flux surface sheets (the interatomic surfaces that arise from the bonds H₄-C₂, C₂-C₃, C₃-C₆, and C₆-H₇) that pass through the narrow opening between those two atoms undergo severe distortions in order to avoid mutual crossing (see ref. 8 for a display of selected zero-flux surface sheets in the acrolein molecule). These distortions markedly reduce the values of the atomic similarity index for the hydrogens in question. Thus, whereas the congestion-free H₅ and H₈ atoms are 99.33% similar, the atomic similarities for the H₄-H₅ and H₄-H₈ pairs amount to only 95.25 and 95.47%, respectively (Table III). The hydrogen H₇ appears to be less affected by steric interactions, as indicated by its 98.31% similarity to H₅ and 98.86% similarity to H₈. The different degrees

TABLE II.
Similarities (%) between Oxygen Atoms in Selected Carbonyl Compounds.^a

	HCHO	CH ₃ CHO	CH ₃ COCH ₃	CH ₂ CHCHO	NH ₂ CHO
CH ₃ CHO	99.87				
CH ₃ COCH ₃	99.69	99.80			
CH ₂ CHCHO	99.82	99.89 (99.74)	99.76		
NH ₂ CHO	99.74	99.74 (99.63)	99.57	99.80 (99.65)	
CO ₂	98.80	98.71	98.56	98.73	98.91

^a The data pertinent to the secondary maxima are listed in parentheses.

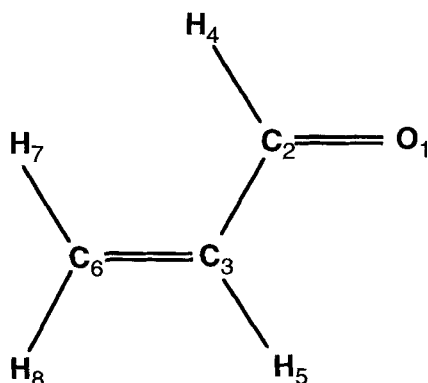


FIGURE 1. Atom numbering in the acrolein molecule. The planar geometry (C_s) of the trans isomer corresponds to the global energy minimum at the MP2/6-311G** level of theory.

of distortion in the atomic surfaces of H₄ and H₇ are reflected in the computed 96.42% similarity between these two atoms.

The congestion-induced distortions influence the atomic properties, such as charge and the kinetic energy, of the hydrogens H₄ and H₇ (Table III). However, in general, atomic properties are affected by multiple factors, such as charge transfer and conjugation. For this reason, their usefulness

as indicators of steric interactions is quite limited. On the other hand, shapes of atoms in molecules reflect mostly atomic connectivities and steric repulsions.

Conclusions

The introduction of analytical representations for the zero-flux surface sheets has opened an avenue to highly accurate, yet computationally efficient, calculations of diverse properties of atoms in molecules. The use of these representations in atomic shape analysis substantially improves the accuracy of the computed similarity indices without increasing the cost of their evaluation. The availability of inexpensive analytical gradients greatly facilitates the maximization of the similarity index with respect to the mutual orientation of the atoms under comparison.

The increased accuracy of atomic similarity calculations enhances their usefulness in diverse aspects of chemical research. The ability to discern and quantify the subtle alterations of atomic shapes that accompany small changes in molecular environment makes quantitative taxonomy of atoms in molecules possible. The unique alignments of

TABLE III.
Properties of Hydrogen Atoms in the Acrolein Molecule.

Atom ^a	Charge	Kinetic Energy (a.u.)	Similarity (%) to the Atom ^{a,b}		
			H ₄	H ₅	H ₇
H ₄	-0.0011	0.6203			
H ₅	0.0538	0.5964	95.25 (94.93)		
H ₇	0.0362	0.6030	96.42 (95.33)	98.31 (98.19)	
H ₈	0.0466	0.6003	95.47 (95.35)	99.33 (98.94)	98.86 (98.22)

^a See Fig. 1 for atom numbering.

^b The data pertinent to the secondary maxima are listed in parentheses.

atoms in molecules, produced by the maximization of the similarity index, are bound to find several applications in the construction of additive schemes for the estimation of multipole moments and (hyper)polarizabilities of large molecules.

Acknowledgments

This work was partially supported by the National Science Foundation under the grant CHE-9224806 and the U.S. Department of Energy through its Supercomputer Computations Research Institute. One of the authors (P. C.) thanks the Catalan Government for his doctoral grant OA/au BQF93/24.

References

1. R. F. W. Bader, *Atoms in Molecules: A Quantum Theory*, Clarendon Press, Oxford, 1990.
2. R. F. W. Bader, A. Larouche, C. Gatti, M. T. Carroll, P. J. MacDougall, and K. B. Wiberg, *J. Phys. Chem.*, **87**, 1142 (1987).
3. C. Chang and R. F. W. Bader, *J. Phys. Chem.*, **96**, 1654 (1992).
4. C. M. Breneman, personal communication, 1994.
5. P. G. Mezey, *J. Comput. Chem.*, **8**, 462 (1987); P. G. Mezey, *J. Math. Chem.*, **2**, 299, 325 (1988).
6. J. Cioslowski and A. Nanayakkara, *J. Amer. Chem. Soc.*, **115**, 11213 (1993).
7. J. Cioslowski and B. B. Stefanov, *Mol. Phys.*, **84**, 707 (1995).
8. B. B. Stefanov and J. Cioslowski, *J. Comput. Chem.*, **16**, 1394 (1995).
9. J. Cioslowski, A. Nanayakkara, and M. Challacombe, *Chem. Phys. Lett.*, **203**, 137 (1993).
10. R. Fletcher, *Comput. J.*, **13**, 317 (1970); D. Goldfarb, *Math. Comput.*, **24**, 23 (1970); D. F. Shanno, *Math. Comput.*, **24**, 647 (1970); C. G. Broyden, *Math. Comput.*, **21**, 368 (1967).
11. B. B. Stefanov and J. Cioslowski, *Can. J. Chem.*, in press.
12. I. Riess and W. Münch, *Theor. Chim. Acta*, **58**, 295 (1981).
13. R. F. W. Bader and P. Becker, *Chem. Phys. Lett.*, **148**, 452 (1988).